

Pareto Characterization of the Multicell MIMO Performance Region With Simple Receivers

Emil Björnson, *Member, IEEE*, Mats Bengtsson, *Senior Member, IEEE*, and Björn Ottersten, *Fellow, IEEE*

Abstract—We study the performance region of a general multicell downlink scenario with multiantenna transmitters, hardware impairments, and low-complexity receivers that treat interference as noise. The Pareto boundary of this region describes all efficient resource allocations, but is generally hard to compute. We propose a novel explicit characterization that gives Pareto optimal transmit strategies using a set of positive parameters—fewer than in prior work. We also propose an implicit characterization that requires even fewer parameters and guarantees to find the Pareto boundary for every choice of parameters, but at the expense of solving quasi-convex optimization problems. The merits of the two characterizations are illustrated for interference channels and ideal network multiple-input multiple-output (MIMO).

Index Terms—Beamforming, dynamic cooperation clusters, fairness-profile, hardware impairments, network MIMO, parametrizations, Pareto boundary, performance region.

I. INTRODUCTION

Interference limits the performance of multicell systems. Conventionally, interference is managed by dividing the available frequency resources such that adjacent cells use different subcarriers. In modern multiantenna systems, interference can instead be managed spatially [1], potentially leading to large improvements through global reuse of all frequency resources. However, spatial interference management requires reliable channel state information (CSI) and joint transmission optimization across cells. This coordination is termed *network MIMO* or *coordinated multi-point* (CoMP).

Multicell performance optimization is more involved than oblivious single-cell optimization; user-fairness and inter-user interference bring a strong intercell coupling. All achievable combinations of user throughput are ideally described by the capacity region, derived in [2] when all base stations act as a single transmitter. In practice, the capacity region is an optimistic performance measure as it, for example, relies on global transceiver design and complex signal processing. Herein, we consider an alternative that we call the *performance region* with simple receivers that treat co-user interference as noise and have a single effective antenna.¹ These assumptions recognize the low-complexity constraints on practical user terminals.

The performance region is characterized by its *Pareto boundary*, a subset of the outer boundary where the performance cannot be

improved for any user without degrading for others. This boundary represents all efficient resource allocations. In general, it is hard to find points on the Pareto boundary, but there are characterizations that reduces the search-space to a few parameters. Some characterizations are *explicit*, thus they provide closed-form transmit strategies based on the parameters [3]–[8]. Their downside is that they only provide necessary conditions; not all parameter choices achieve the Pareto boundary. On the contrary, *implicit* characterizations guarantee that a point on the outer boundary is found [8]–[11], but a quasi-convex problem must be solved for each choice of parameter values to find the corresponding transmit strategy.

Explicit Pareto characterizations for general multicell systems with K_t transmitters and K_r users were given in [3] and [4]. Both required $K_t(K_r - 1)$ parameters for beamforming (and often additional power-control parameters), and these were improved from complex-valued in [3] to $[0, 1]$ -parameters in [4]. The special case of the multiple-input single-output (MISO) interference channel, where each transmitter serves a single unique user, has received particular attention. A characterization with $K_t(K_r - 1)$ complex-valued parameters was derived in [5] and it was improved in [6] to $[0, 1]$ -parameters. A similar² characterization was proposed in [8], although closed-form beamforming is not guaranteed. Recently, [7] showed that only a single parameter is required for the two-user MISO interference channel (and it even ensures attaining the Pareto boundary).

Implicit Pareto characterizations have received considerably less attention. The broadcast capacity region was considered in [9], and the performance region of MISO interference channels in [8], [10]. In both cases, $K_r - 1$ parameters were used to define a ray from the origin. The intersection between this ray and the outer boundary of the region was formulated as a quasi-convex optimization problem. There are connections to the optimization of worst-user performance [11], [12], which represents a certain ray direction.

Herein, we consider a general multicell scenario with dynamic cooperation clusters [13], basically describing anything from interference channels to ideal network MIMO in a unified manner. The performance is measured by arbitrary functions of the single-to-noise-and-interference ratios (SINRs), we consider arbitrary linear power constraints and hardware impairments. The main contributions are as follows.

- A novel explicit Pareto boundary characterization is proposed. It exploits the idea of uplink-downlink duality [12]–[14] and uses $K_r + L - 2$ positive parameters, where L is the number of power constraints. Thus, it requires fewer parameters than the prior work in [3]–[6], [8].
- The implicit Pareto boundary characterizations in [8]–[11] are extended to general multicell scenarios, using $K_r - 1$ parameters in the interval $[0, 1]$. Each point is given by solving a quasi-convex optimization problem.
- The proposed characterizations include physical hardware impairments that could distort the transmitted signals, while the prior work in [1]–[16] are limited to ideal transceiver hardware.

Copyright (c) 2012 IEEE. Personal use of this material is permitted. However, permission to use this material for any other purposes must be obtained from the IEEE by sending a request to pubs-permissions@ieee.org. The associate editor coordinating the review of this manuscript and approving it for publication was Dr. Milica Stojanovic. The research leading to these results has received funding from the European Research Council under the European Community's Seventh Framework Programme (FP7/2007-2013) / ERC grant agreement number 228044.

E. Björnson and M. Bengtsson are with the Signal Processing Laboratory, ACCESS Linnaeus Center, KTH Royal Institute of Technology, SE-100 44 Stockholm, Sweden (e-mail: emil.bjornson@ee.kth.se; mats.bengtsson@ee.kth.se).

B. Ottersten is with the Signal Processing Laboratory, ACCESS Linnaeus Center, KTH Royal Institute of Technology, SE-100 44 Stockholm, Sweden. He is also with the Interdisciplinary Centre for Security, Reliability and Trust (SnT), University of Luxembourg, 6 rue Richard Coudenhove-Kalergi, L-1359 Luxembourg-Kirchberg, Luxembourg (email: bjorn.ottersten@ee.kth.se).

Digital Object Identifier 10.1109/TSP.2012.2199309

¹It is usually called the *rate region* in prior work, but also other performance measures than the achievable data rate are considered herein.

²Positive parameters are used in [8], but there are bijective functions from $[0, \infty)$ to $[0, 1]$ making the complexity identical.

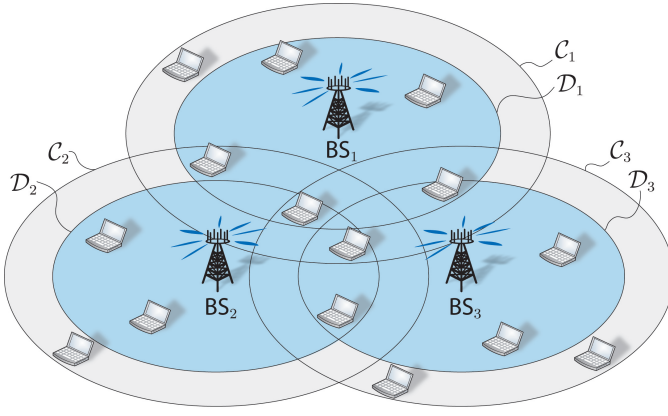


Fig. 1. Schematic intersection between three cells. BS_j serves users in the inner circle (\mathcal{D}_j), while it coordinates interference to users in the outer circle (\mathcal{C}_j). Ideally, negligible interference is caused to users outside both circles.

II. SYSTEM MODEL AND PRELIMINARIES

We consider downlink transmission with K_t base stations and K_r users. The j th base station is denoted BS_j and has N_j antennas. The k th user is denoted MS_k and is a simple receiver.

Definition 1. A simple receiver has the following characteristics:

- It is viewed to have single effective antenna in the transmit optimization;
- It treats co-user interference as noise (i.e., without trying to decode and subtract interfering signals).

The first property means that MS_k either has a single antenna or has $M_k > 1$ antennas that are combined into a single effective antenna (using receive combining) prior to transmit optimization to enable practical non-iterative transmission design. The second property means single user detection and enables low-complexity reception, but is suboptimal except in some low-interference regimes [15].

In a general multicell scenario, some users are served in a coordinated manner by multiple transmitters. In addition, some transmitters and receivers are very far apart, making it hard to estimate these channels and pointless to use such uncertain estimates for interference coordination. To capture these properties and enable unified analysis, we adopt the dynamic coordination framework of [13].

Definition 2. Dynamic cooperation clusters means that BS_j has the following characteristics:

- It has perfect CSI to receivers in $\mathcal{C}_j \subseteq \{1, \dots, K_r\}$, while interference generated to receivers $\bar{k} \notin \mathcal{C}_j$ are treated as additive complex Gaussian noise;
- It serves the receivers in $\mathcal{D}_j \subseteq \mathcal{C}_j$ with data.

This coordination framework is characterized by the sets $\mathcal{C}_j, \mathcal{D}_j$, and the mnemonic rule is that \mathcal{D}_j describes *data* from transmitter j while \mathcal{C}_j describes *coordination* from transmitter j . To reduce backhaul signaling of data, the cardinality of \mathcal{D}_j is typically smaller than that of \mathcal{C}_j . These sets are illustrated in Fig. 1 and can be selected based on long-term channel gains (see [13] for details). Special cases include ideal network MIMO where all transmitters serve all users (with $\mathcal{C}_j = \mathcal{D}_j = \{1, \dots, K_r\}$) and the interference channel (with $K_t = K_r$, $\mathcal{D}_j = \{j\}$, and $\mathcal{C}_j = \{1, \dots, K_r\}$). More detailed examples are available in [11] and [13].

To enable coordinated transmissions, perfect phase coherence and synchronous interference is assumed between transmitters that serve users jointly (cf. [16]). The effective flat fading channel from BS_j to MS_k is denoted \mathbf{h}_{jk} . The combined effective channel from all

transmitters is denoted $\mathbf{h}_k = [\mathbf{h}_{1k}^T \dots \mathbf{h}_{K_t k}^T]^T \in \mathbb{C}^{N \times 1}$ with $N = \sum_{j=1}^{K_t} N_j$. The received signal at MS_k is modeled as

$$y_k = \mathbf{h}_k^H \mathbf{C}_k \left(\sum_{\bar{k}=1}^{K_r} \mathbf{D}_{\bar{k}} \mathbf{s}_{\bar{k}} + \boldsymbol{\xi} \right) + n_k \quad (1)$$

where \mathbf{D}_k selects the transmit antennas that send the zero-mean data signal $\mathbf{s}_k \in \mathbb{C}^{N \times 1}$ to MS_k . The signal correlation matrix $\mathbf{S}_k = \mathbb{E}\{\mathbf{s}_k \mathbf{s}_k^H\}$ is a parameter in the transmission design.

Let $\mathbf{I}_M, \mathbf{0}_M \in \mathbb{C}^{M \times M}$ denote identity and zero matrices, respectively. Then, $\mathbf{D}_k \in \mathbb{C}^{N \times N}$ is block-diagonal and the j th block is \mathbf{I}_{N_j} if $k \in \mathcal{D}_j$ and $\mathbf{0}_{N_j}$ if $k \notin \mathcal{D}_j$. Similarly, $\mathbf{C}_k \in \mathbb{C}^{N \times N}$ selects signals from transmitters with non-negligible channels to MS_k ; $\mathbf{C}_k \in \mathbb{C}^{N \times N}$ is block-diagonal and the j th block is \mathbf{I}_{N_j} if $k \in \mathcal{C}_j$ and $\mathbf{0}_{N_j}$ if $k \notin \mathcal{C}_j$. The remaining (weak) interference and thermal noise is modeled by $n_k \in \mathcal{CN}(0, \sigma_k^2)$.

In contrast to the prior works [1]–[16], we consider that physical transceivers suffer from hardware impairments (e.g., nonlinear amplifiers, phase noise, and IQ-imbalance) [17]–[19]. The transmitter impairments are well-modeled by the Gaussian distortion term $\boldsymbol{\xi} \in \mathcal{CN}(\mathbf{0}, \boldsymbol{\Xi})$ [17]. The covariance matrix $\boldsymbol{\Xi} \in \mathbb{C}^{N \times N}$ is assumed diagonal and the distortion power at the n th antenna is proportional to the transmit power at this antenna: $\boldsymbol{\Xi} = \sum_{n=1}^N \sum_{k=1}^{K_r} \mathbf{T}_n \mathbf{D}_k \mathbf{S}_k \mathbf{D}_k^H \mathbf{T}_n^H$, where the n th diagonal-element of \mathbf{T}_n is κ_n while all other elements are zero. The proportionality constant κ_n is known as the error vector magnitude (EVM) and typically satisfies $\kappa_n \in [0, 0.15]$, depending on the quality of the transmitter hardware.

A. Power Constraints

The transmission is limited by L linear power constraints

$$\sum_{k=1}^{K_r} \text{tr}\{\mathbf{Q}_{lk} \mathbf{S}_k\} \leq q_l, \quad l = 1, \dots, L, \quad (2)$$

where $\mathbf{Q}_{lk} \in \mathbb{C}^{N \times N}$ are Hermitian positive semi-definite matrices for all l, k . To ensure that the total power is constrained and only is allocated to dimensions used for transmission, these matrices must satisfy two conditions: a) $\mathbf{Q}_{lk} - \mathbf{D}_k^H \mathbf{Q}_{lk} \mathbf{D}_k$ is diagonal and b) $\sum_{l=1}^L \mathbf{Q}_{lk} \succ \mathbf{0}_N \forall k$.

A total power constraint ($L = 1$) as well as per-base station ($L = K_t$) and per-antenna constraints ($L = N$) can be expressed as (2); see examples in [13]. The matrices \mathbf{Q}_{lk} could be identical among users served by the same set of base stations, but it is also possible to have user-specific or area-specific soft-shaping constraints that limit the interference generated in certain channel subspaces identified by \mathbf{Q}_{lk} (e.g., to not disturb neighboring systems [20]).

B. Performance Region

Most common quality measures are monotonic functions of the signal-to-interference-and-noise ratio (SINR); for example, achievable data rate, mean square error (MSE), and bit/symbol error rate (BER/SER). For the system model in (1), the SINR at MS_k becomes³

$$\text{SINR}_k(\mathbf{S}_1, \dots, \mathbf{S}_{K_r}) = \frac{\mathbf{h}_k^H \mathbf{D}_k \mathbf{S}_k \mathbf{D}_k^H \mathbf{h}_k}{\sigma_k^2 + \mathbf{h}_k^H \mathbf{C}_k \left(\sum_{\bar{k} \neq k} \mathbf{D}_{\bar{k}} \mathbf{S}_{\bar{k}} \mathbf{D}_{\bar{k}}^H + \boldsymbol{\Xi} \right) \mathbf{C}_k^H \mathbf{h}_k}. \quad (3)$$

Thus, optimizing the performance means selecting the transmit correlation matrices \mathbf{S}_k appropriately.

³For notational simplicity, dirty-paper coding has not been included. It can however be used to presubtract interference at the transmitter-side, and the corresponding SINR expressions can be achieved using the same approach as in [14].

Herein, we model the performance of MS_k by an arbitrary continuous and strictly increasing monotonic performance function $g_k(\text{SINR}_k)$ that we seek to maximize⁴ for each user. For simplicity, we let $g_k(0) = 0$. We define the region of performance outcomes for feasible transmit correlation matrices $\mathbf{S}_1, \dots, \mathbf{S}_{K_r}$:

Definition 3. The achievable performance region $\mathcal{R} \subset \mathbb{R}_{+}^{K_r}$ is

$$\mathcal{R} = \{ (g_1(\text{SINR}_1), \dots, g_{K_r}(\text{SINR}_{K_r})) : (\mathbf{S}_1, \dots, \mathbf{S}_{K_r}) \in \mathcal{S} \} \quad (4)$$

where the set of feasible transmit strategies is

$$\mathcal{S} = \left\{ (\mathbf{S}_1, \dots, \mathbf{S}_{K_r}) : \mathbf{S}_k \succeq \mathbf{0}_N \ \forall k, \sum_{k=1}^{K_r} \text{tr}\{\mathbf{Q}_{lk}\mathbf{S}_k\} \leq q_l \ \forall l \right\}. \quad (5)$$

This region describes the performance that can be simultaneously achieved by the different users. It is a compact region since \mathcal{S} is compact. The interesting part of \mathcal{R} is a subset of the outer boundary, called the Pareto boundary, where no user can improve its performance without degrading others' performance:

Definition 4. The outer boundary $\partial\mathcal{R}^+ \subseteq \mathcal{R}$ and the Pareto boundary $\partial\mathcal{R} \subseteq \mathcal{R}$ consist of all $\mathbf{r} \in \mathcal{R}$ for which there is no $\mathbf{r}' \in \mathcal{R} \setminus \{\mathbf{r}\}$ with $\mathbf{r}' > \mathbf{r}$ or $\mathbf{r}' \geq \mathbf{r}$, respectively (component-wise inequalities).

All efficient outcomes of performance optimization lie on the Pareto boundary. There are no simple expressions for $\partial\mathcal{R}$, but explicit and implicit characterization are derived in the following sections.

III. EXPLICIT PARETO BOUNDARY CHARACTERIZATION

In this section, we derive a subset of the feasible transmit strategies in \mathcal{S} that can attain the complete Pareto boundary and is explicitly characterized using $K_r + L - 2$ parameters from $[0, 1]$. Recalling that each strategy consists of K_r transmit correlation matrices of size $N \times N$, the derived necessary condition constitutes a major reduction of the search space for Pareto optimal strategies.

We will exploit the sufficiency of single-stream beamforming, proved similarly to [13, Theorem 1]:

Lemma 1. Each point $\mathbf{r} \in \partial\mathcal{R}$ can be attained by some transmit strategy $(\mathbf{S}_1^*, \dots, \mathbf{S}_{K_r}^*) \in \mathcal{S}$ satisfying $\text{rank}(\mathbf{S}_k^*) \leq 1 \ \forall k$.

The lemma says that it is sufficient to consider transmit correlation matrices that are either rank-one or identically zero. Next, we propose such a strategy based on a set of parameters.

Strategy 1. For some given non-negative parameters $\{\mu_k\}_{k=1}^{K_r}$ and $\{\lambda_l\}_{l=1}^L$, let the signal correlation matrix of user k be $\mathbf{S}_k = p_k \mathbf{w}_k \mathbf{w}_k^H$ with

$$\mathbf{w}_k = \frac{\Psi_k^\dagger \mathbf{D}_k^H \mathbf{h}_k}{\|\Psi_k^\dagger \mathbf{D}_k^H \mathbf{h}_k\|} \quad (6)$$

$$[p_1 \dots p_{K_r}] = [\gamma_1 \sigma_1^2 \dots \gamma_{K_r} \sigma_{K_r}^2] \mathbf{M}^\dagger \quad (7)$$

where

$$\Psi_k = \left(\sum_{\bar{k}=1}^{K_r} \frac{\mu_{\bar{k}}}{\sigma_{\bar{k}}^2} \mathbf{D}_{\bar{k}}^H \mathbf{C}_{\bar{k}}^H (\mathbf{h}_{\bar{k}} \mathbf{h}_{\bar{k}}^H + \sum_{n=1}^N \mathbf{T}_n^H \mathbf{h}_{\bar{k}} \mathbf{h}_{\bar{k}}^H \mathbf{T}_n) \mathbf{C}_{\bar{k}} \mathbf{D}_{\bar{k}} \right. \\ \left. + \sum_{l=1}^L \frac{\lambda_l}{q_l} \mathbf{Q}_{lk} \right) \quad (8)$$

$$\gamma_k = \frac{\mu_k}{\sigma_k^2} \mathbf{h}_k^H \mathbf{D}_k (\Psi_k - \frac{\mu_k}{\sigma_k^2} \mathbf{D}_k^H \mathbf{h}_k \mathbf{h}_k^H \mathbf{D}_k)^\dagger \mathbf{D}_k^H \mathbf{h}_k. \quad (9)$$

⁴In case of a strictly monotonic decreasing error measure $\tilde{g}_k(\text{SINR}_k)$ that should be minimized (e.g., MSE, BER, or SER), we can maximize $g_k(\text{SINR}_k) = \tilde{g}_k(0) - \tilde{g}_k(\text{SINR}_k)$ instead.

In (6)-(9), we let $(\cdot)^\dagger$ denote the Moore-Penrose pseudoinverse and the ij th element of $\mathbf{M} \in \mathbb{R}^{K_r \times K_r}$ is

$$[\mathbf{M}]_{ij} = \begin{cases} |\mathbf{h}_i^H \mathbf{D}_i \mathbf{w}_i|^2 - \gamma_i \sum_{n=1}^N |\mathbf{h}_i^H \mathbf{D}_i \mathbf{T}_n \mathbf{w}_i|^2, & i = j, \\ -\gamma_j (|\mathbf{h}_j^H \mathbf{C}_j \mathbf{D}_i \mathbf{w}_i|^2 + \sum_{n=1}^N |\mathbf{h}_j^H \mathbf{C}_j \mathbf{D}_i \mathbf{T}_n \mathbf{w}_i|^2), & i \neq j. \end{cases} \quad (10)$$

The following theorem shows that Strategy 1 can attain any point on the Pareto boundary $\partial\mathcal{R}$ by proper parameter selection.

Theorem 1. Each Pareto optimal point $\mathbf{r} \in \partial\mathcal{R}$ is attained by $(\mathbf{S}_1, \dots, \mathbf{S}_{K_r}) \in \mathcal{S}$ given by Strategy 1 for some selection of the parameters $\{\mu_k\}_{k=1}^{K_r}$ and $\{\lambda_l\}_{l=1}^L$ that satisfies $\sum_{k=1}^{K_r} \mu_k = 1$ and $\sum_{l=1}^L \lambda_l = 1$.

Proof: For brevity, the proof is given in the Appendix. ■

The characterization in Theorem 1 uses $K_r + L$ parameters from $[0, 1]$, but we only need to select $K_r + L - 2$ parameters since the last two are given by the two sum constraints. Observe that our novel characterization only has a single parameter per user, although multiple base stations are involved. This reduces the number of parameters compared with the prior work in [3]–[6] and [8], where each transmitter has its own parameter for each user. The parameters μ_k, λ_l implicitly determine beamforming directions and power allocation. The direction \mathbf{w}_k in (6) is created by rotating maximum ratio transmission $\mathbf{D}_k^H \mathbf{h}_k$ using the matrix Ψ_k , whose terms determine to which extent power constraints, co-user interference, and hardware distortion are taken into account. These terms are weighted by μ_k, λ_l and their impact is showed next.

Corollary 1. If $g_k(\cdot)$ is differentiable, changing the parameters in Theorem 1 impacts the performance of MS_k as follows:

$$\begin{aligned} \frac{\partial}{\partial \mu_{\bar{k}}} g_k(\text{SINR}_k) & \begin{cases} \geq 0, & k = \bar{k}, \\ \leq 0, & k \neq \bar{k}, \end{cases} \\ \frac{\partial}{\partial \lambda_l} g_k(\text{SINR}_k) & \leq 0 \quad \forall l. \end{aligned} \quad (11)$$

Proof: Observe that Strategy 1 gives $\text{SINR}_k = \gamma_k$. Differentiation of the γ_k -expression in Strategy 1 proves the corollary, in conjunction with the monotonicity of $g_k(\cdot)$. ■

The corollary proves that increasing μ_k improves the performance for MS_k and degrades it for other users, thus μ_k represents the system priority of MS_k . The level of enforcement of the l th power constraint is determined by λ_l and should be small to boost performance; λ_l is zero for inactive constraints. It is non-trivial which parameters to modify to improve system performance and fulfill all constraints. In fact, it is unlikely to find Pareto optimal points by trial-and-error selection. However, close-to-optimal performance is relatively easy to achieve—the well-known signal-to-leakage-and-noise ratio (SLNR) beamforming [16] and distributed virtual SINR (DVSINR) beamforming [3] are achieved by simple parameter selections.

Strategy 1 will not produce feasible strategies for all parameter selections, but this is easily arranged.

Strategy 2. Let $(\mathbf{S}_1, \dots, \mathbf{S}_{K_r})$ be suggested by Strategy 1. The modified strategy with $\tilde{\mathbf{S}}_k = \mathbf{S}_k / c \ \forall k$ and $c = \max_l (\sum_k \text{tr}\{\mathbf{Q}_{lk}\mathbf{S}_k\} / q_l)$ will always be feasible.

This modification only affects suboptimal and infeasible strategies since Pareto optimal strategies have $c = 1$ (i.e., satisfy at least one constraint with equality, see [13, Theorem 2]).

IV. IMPLICIT PARETO BOUNDARY CHARACTERIZATION

The explicit characterization in Section III reduces the search-space for Pareto optimal points, but not all parameter selections attain the Pareto boundary. Next, we provide an implicit characterization that

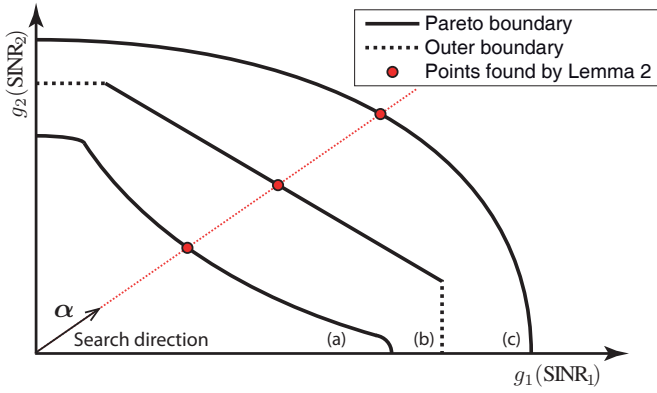


Fig. 2. Example of performance regions: (a) is non-convex and (b), (c) are convex. The outer boundary and Pareto boundary are identical, except in Case (b). The search direction α of the implicit characterization is shown along with the Pareto optimal points that it will find.

provides a point on the outer boundary for *every* parameter selection, but at the expense of solving a quasi-convex optimization problem. As pointed out in Definition 4, the Pareto boundary is only a subset of the outer boundary. However, they are equal in many multicell scenarios; three examples are given in Fig. 2 and only the flat parts (those orthogonal to an axis) in Case (b) are not Pareto optimal.

The approach used herein is based on *fairness-profiles* [11], which is a conceptual extension of the rate-profile approach in [9] where users achieve pre-defined portions of the sum performance. We use $K_r - 1$ parameters to define a fairness-profile $\alpha = [\alpha_1, \dots, \alpha_{K_r}] \in \mathbb{R}^{K_r}$ with non-negative entries and unit L_1 -norm (thus, the last entry is given as $\alpha_{K_r} = 1 - \sum_{k=1}^{K_r-1} \alpha_k$). This vector points out the direction in which we search for the outer boundary; see Fig. 2. The corresponding optimization problem is formulated as

$$\begin{aligned} & \underset{g_{\text{sum}}, (\mathbf{S}_1, \dots, \mathbf{S}_{K_r}) \in \mathcal{S}}{\text{maximize}} && g_{\text{sum}} \\ & \text{subject to} && g_k(\text{SINR}_k) = \alpha_k g_{\text{sum}} \quad \forall k. \end{aligned} \quad (12)$$

This problem might seem difficult, but since single-stream beamforming can be used (see Lemma 1) it can be formulated as quasi-convex. By setting $\mathbf{h}_k^H \mathbf{D}_k \mathbf{v}_k > 0$ (without loss of generality) and using bisection techniques [21], it can be solved with linear convergence as a series of convex feasibility problems:

Lemma 2. The solution to (12) can be achieved by bisection over the range $\mathcal{G} = [0, g_{\text{max}}]$ of values for g_{sum} . For a given $g_{\text{candidate}} \in \mathcal{G}$, the convex feasibility problem

$$\begin{aligned} & \text{find } \mathbf{v}_1, \dots, \mathbf{v}_{K_r} \\ & \text{subject to } \sum_{k=1}^{K_r} \mathbf{v}_k^H \mathbf{Q}_{lk} \mathbf{v}_k \leq q_l \quad \forall l, \\ & \quad \Im\{\mathbf{h}_k^H \mathbf{D}_k \mathbf{v}_k\} = 0 \quad \forall k, \\ & \quad \sqrt{\sigma_k^2 + \sum_{\bar{k} \neq k} |\mathbf{h}_{\bar{k}}^H \mathbf{C}_{\bar{k}} \mathbf{D}_{\bar{k}} \mathbf{v}_{\bar{k}}|^2 + \sum_{k=1}^{K_r} \sum_{n=1}^N |\mathbf{h}_k^H \mathbf{C}_{\bar{k}} \mathbf{D}_{\bar{k}} \mathbf{T}_n \mathbf{v}_{\bar{k}}|^2} \\ & \quad \leq \frac{1}{\sqrt{\gamma_k}} \mathbf{h}_k^H \mathbf{D}_k \mathbf{v}_k \quad \forall k \end{aligned} \quad (13)$$

is solved for $\gamma_k = g_k^{-1}(\alpha_k g_{\text{candidate}})$. If there exist feasible solutions, all $g \in \mathcal{G}$ with $g < g_{\text{candidate}}$ are removed from \mathcal{G} . Otherwise, all $g \in \mathcal{G}$ with $g \geq g_{\text{candidate}}$ are removed from \mathcal{G} .

The initial upper bound can, for instance, be selected as $g_{\text{max}} = \sum_{k=1}^{K_r} g_k(\|\mathbf{D}_k^H \mathbf{h}_k\|^2 / (\nu_k \sigma_k^2))$ where $1/\nu_k$ is an upper bound on the

transmit power and is the smallest strictly positive eigenvalue of $\frac{\mathbf{D}_k^H \mathbf{Q}_{lk} \mathbf{D}_k}{q_l \text{tr}(\mathbf{D}_k)}$ among all l .

In a practical implementation, this algorithm halves the range \mathcal{G} (by testing the feasibility at midpoints) until it is smaller than some pre-defined accuracy. The feasibility problem in (13) is a second order cone program and thus solvable in polynomial time using software packages such as CVX [22]. The implicit parametrization is established by the following theorem.

Theorem 2. Each point on the outer boundary (and Pareto boundary) is achieved by Lemma 2 for a *unique* α with unit L_1 -norm and non-negative entries. Each such α gives a point on the outer boundary.

Proof: For brevity, the proof is given in the Appendix. ■

A similar characterization was proposed in [8] and [10] for MISO interference channels, thus we extend the previous work to arbitrary multicell scenarios with arbitrary linear power constraints and hardware impairments. The fairness-profile optimization in (12) is also a solution to maximize $\min_k g_k(\text{SINR}_k) / \alpha_k$, which can be viewed as optimizing the weighted worst-user performance. The special case of $\alpha_k = 1/K_r \quad \forall k$ corresponds to classic worst-user optimization; see, for example, [11], [12].

V. TWO SIMPLE MULTICELL EXAMPLES

Next, we exemplify the characterizations on two simple multicell scenarios that can be described by our general framework.

A. MISO Interference Channel

The Pareto boundary when BS_j only transmits to MS_j (i.e., $K_t = K_r$) has attracted much attention under per-base station power constraints [5]–[8]. The state-of-the-art Pareto characterizations require $K_t(K_r - 1)$ parameters, while Theorem 1 uses $2K_r - 2$ parameters under these conditions. Thus, our novel characterization is advantageous whenever $K_r \geq 3$, and the benefit increases rapidly with K_r . In the special case of $K_r = 2$, recent work in [7] only requires a single parameter; a similar reduction is not possible in our general multicell characterization without removing the support for arbitrary power constraints.

In Fig. 3, the performance region is shown for a uncorrelated Rayleigh fading channel realization with $K_t = K_r = 3$, $N_t = 4$, $\kappa_n = 0$, and an average SNR of 10 dB (for maximum ratio transmission). The data rate $g_k(\text{SINR}_k) = \log_2(1 + \text{SINR}_k)$ is used as performance measure and the performance region is generated with Strategy 2 by changing the four parameters in steps of 0.02 and filling the space between the achieved points. The region looks like a box with rounded edges, and the color bar shows the sum rate.

B. Ideal Network MIMO

In this scenario, all base stations send data to all users and have (identical) per-antenna power constraints as in [14]. The performance region for this scenario has not been characterized in prior work.

We illustrate performance regions in a scenario with $N = 3$ and two single-antenna users. An uncorrelated Rayleigh fading channel realization is used at an average SNR of 10 dB. The region with $g_k(\text{SINR}_k) = \log_2(1 + \text{SINR}_k)$ is shown in Fig. 4 for ideal hardware. The shaded area is attained by Strategy 2 when the three parameters are varied in steps of 0.01. The outer boundary of this area coincides with the plotted Pareto boundary, computed by Lemma 2 using a grid of α vectors. The maximal sum rate and fairness (i.e., $g_1 = g_2$) points are shown, along with the corresponding points under zero-forcing beamforming (based on [23]). The same region is shown in Fig. 5 with impairments: $\kappa_n \in \{0, 0.05, 0.1, 0.15, 0.2\}$. The sum rate loss is 0.2% – 13.5% depending the level of impairments and

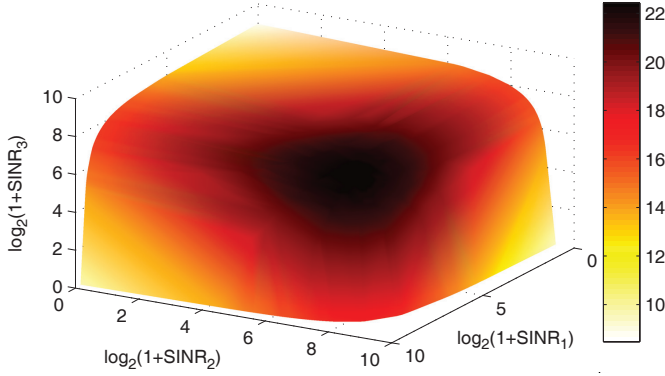


Fig. 3. Rate region (at SNR 10 dB) for a three-user MISO interference channel with four antennas per transmitter, ideal hardware, and per-base station constraints. The color bar shows the sum rate.

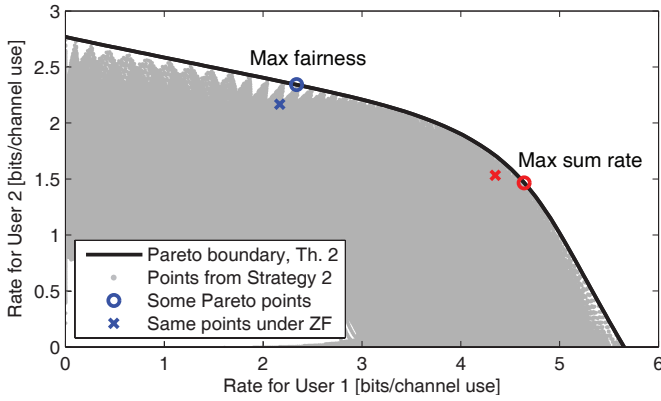


Fig. 4. Rate region (at SNR 10 dB) for ideal network MIMO with two users, three transmit antennas, ideal hardware, and per-antenna constraints.

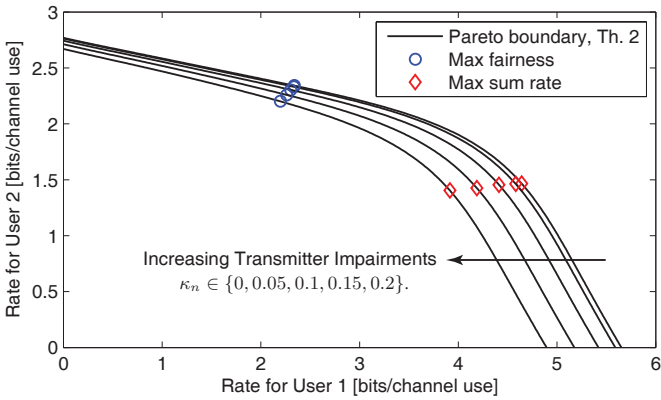


Fig. 5. Rate region (at SNR 10 dB) for the same scenario and channel realization as in Fig. 4, but with varying transmitter impairments: $\kappa_n \in \{0, 0.05, 0.1, 0.15, 0.2\}$.

which part of the boundary we consider; User 1 is more sensitive to impairments as this user has a stronger channel than User 2.

In Fig. 6, the symbol error rates (SERs) with 4-QAM are shown for the same channel realization. The minimal sum SER and maximal fairness are shown along with the same zero-forcing points as in Fig. 4. Comparing the two performance measures, the maximal fairness points have the same interpretations in both cases while optimizing sum performance yields very different results.

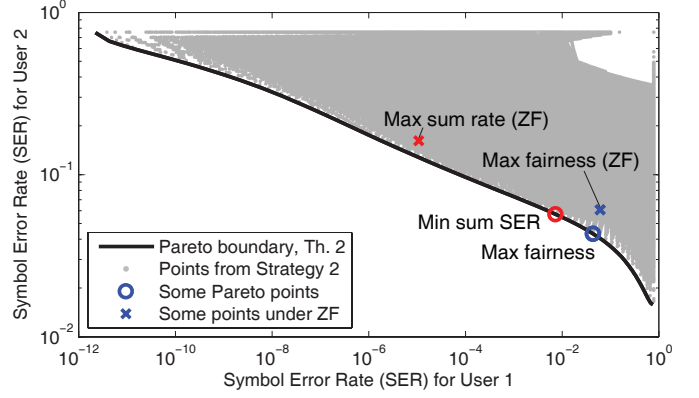


Fig. 6. Symbol error rate (SER) region (at SNR 10 dB) for ideal network MIMO with two users, three transmit antennas, ideal hardware, and per-antenna constraints.

VI. CONCLUSION

Efficient resource allocation is necessary to achieve the full potential of multicell multiantenna communication. We considered a general setup where K_t transmitters serve K_r users under dynamic cooperation clusters, L arbitrary power constraints, and practical hardware impairments. The Pareto boundary of the performance region describes all efficient resource allocations. A novel explicit characterization of the Pareto boundary was proposed that gives Pareto optimal transmit strategies in closed-form using $K_r + L - 2$ parameters between zero and one (instead of $K_t(K_r - 1)$ as in prior work). We also extended previous work on implicit characterizations where each set of parameters guarantees to find a point on the Pareto boundary, but at the expense of solving a quasi-convex optimization problem to find the corresponding transmit strategy.

APPENDIX

Proof of Theorem 1: For each given $\mathbf{r} = [r_1, \dots, r_{K_r}] \in \partial\mathcal{R}$, Lemma 1 states that it is sufficient to consider rank-one solutions with $\mathbf{S}_k = \tilde{\mathbf{w}}_k \tilde{\mathbf{w}}_k^H$. Observe that the optimal solution also solves the convex feasibility problem in (13) when $\gamma_k = g_k^{-1}(r_k)$. Using Lagrange multipliers $\{\mu_k\}_{k=1}^{K_r}$ and $\{\lambda_l\}_{l=1}^L$, the Lagrangian of (13) can be expressed as (similarly to [14, Proof of Proposition 1])

$$\mathcal{L} = \sum_{k=1}^{K_r} \mu_k - \sum_{l=1}^L \lambda_l + \sum_{k=1}^{K_r} \tilde{\mathbf{w}}_k^H \left(\Psi_k - \frac{\mu_k}{\sigma_k^2} \left(1 + \frac{1}{\gamma_k} \right) \mathbf{D}_k^H \mathbf{h}_k \mathbf{h}_k^H \mathbf{D}_k \right) \tilde{\mathbf{w}}_k. \quad (14)$$

The stationarity of the optimal $\tilde{\mathbf{w}}_k$ (i.e., $\partial\mathcal{L}/\partial\tilde{\mathbf{w}}_k = \mathbf{0}$) and multiplication with the Moore-Penrose pseudoinverse of Ψ_k gives

$$\tilde{\mathbf{w}}_k = \underbrace{\Psi_k^\dagger \mathbf{D}_k^H \mathbf{h}_k \frac{\mu_k}{\sigma_k^2} \left(1 + \frac{1}{\gamma_k} \right) \mathbf{h}_k^H \mathbf{D}_k}_{=\text{scalar}} \tilde{\mathbf{w}}_k. \quad (15)$$

Since the phase of $\tilde{\mathbf{w}}_k$ will not affect the Lagrangian, $\tilde{\mathbf{w}}_k$ can without loss of optimality be expressed as $\tilde{\mathbf{w}}_k = \sqrt{p_k} \mathbf{w}_k$ with \mathbf{w}_k as in (6) and for some $p_k \geq 0$. To determine p_k for $k = 1, \dots, K_r$, observe that since the solution lies on the Pareto boundary, all SINR constraints in (13) are satisfied with equality. The achieved SINRs γ_k are found by multiplying (15) with $\mathbf{h}_k^H \mathbf{D}_k$ from the left and then divide by $\mathbf{h}_k^H \mathbf{D}_k \tilde{\mathbf{w}}_k$. The SINR equalities give K_r linear equations that can be expressed and solved as in (6).

Finally, observe that (14) (and all equations in Strategy 1) is unaffected by a common scaling of all Lagrange multipliers, thus we can assume $\sum_{k=1}^{K_r} \mu_k + \sum_{l=1}^L \lambda_l = 2$ without losing any solutions. Also observe that $\sum_{k=1}^{K_r} \mu_k - \sum_{l=1}^L \lambda_l$ is the dual function and

it is zero at the optimum due to the strong duality of (13). The combination of these two constraints gives that $\sum_{k=1}^{K_r} \mu_k = 1$ and $\sum_{l=1}^L \lambda_l = 1$.

Proof of Theorem 2: Geometrically, (12) searches for the outer boundary along a ray from the origin in the direction of α . To prove the first statement, observe that a ray can always be drawn to any outer boundary point, but the uniqueness of this ray requires a proof. Say that the (outmost) intersection of a certain ray with the outer boundary is $\bar{\mathbf{r}}$, using the strategy $\mathbf{S}_k = \bar{p}_k \mathbf{w}_k \mathbf{w}_k^H \forall k$ with $\|\bar{\mathbf{w}}_k\| = 1$. Observe that every $\gamma = [\gamma_1, \dots, \gamma_{K_r}]^T \geq \mathbf{0}$ with $\gamma < \bar{\mathbf{r}}$ can be achieved by using the strategy $\mathbf{S}'_k = p_k \mathbf{w}_k \mathbf{w}_k^H \forall k$ with p_k given by (6) (the existence of such p_k and that $p_k \leq \bar{p}_k$ is easily shown using interference functions [24, Section 3]). Thus, all $\gamma < \bar{\mathbf{r}}$ belong to the interior of \mathcal{R} and therefore the ray can only intersect the outer boundary once. The second part follows from the compactness of \mathcal{R} .

ACKNOWLEDGEMENT

The authors would like to thank P. Zetterberg for sharing his knowledge on hardware impairments.

REFERENCES

- [1] D. Gesbert, S. Hanly, H. Huang, S. Shamai, O. Simeone, and W. Yu, "Multi-cell MIMO cooperative networks: A new look at interference," *IEEE J. Sel. Areas Commun.*, vol. 28, no. 9, pp. 1380–1408, 2010.
- [2] H. Weingarten, Y. Steinberg, and S. Shamai, "The capacity region of the Gaussian multiple-input multiple-output broadcast channel," *IEEE Trans. Inf. Theory*, vol. 52, no. 9, pp. 3936–3964, 2006.
- [3] E. Björnson, R. Zakhour, D. Gesbert, and B. Ottersten, "Cooperative multicell precoding: Rate region characterization and distributed strategies with instantaneous and statistical CSI," *IEEE Trans. Signal Process.*, vol. 58, no. 8, pp. 4298–4310, 2010.
- [4] R. Mochaourab and E. Jorswieck, "Optimal beamforming in interference networks with perfect local channel information," *IEEE Trans. Signal Process.*, vol. 59, no. 3, pp. 1128–1141, 2011.
- [5] E. Jorswieck, E. Larsson, and D. Danev, "Complete characterization of the Pareto boundary for the MISO interference channel," *IEEE Trans. Signal Process.*, vol. 56, no. 10, pp. 5292–5296, 2008.
- [6] X. Shang, B. Chen, and H. V. Poor, "Multiuser MISO interference channels with single-user detection: Optimality of beamforming and the achievable rate region," *IEEE Trans. Inf. Theory*, vol. 57, no. 7, pp. 4255–4273, 2011.
- [7] R. Mochaourab and E. Jorswieck, "Exchange economy in two-user multiple-input single-output interference channels," *IEEE J. Sel. Topics Signal Process.*, vol. 6, no. 2, pp. 151–164, 2012.
- [8] R. Zhang and S. Cui, "Cooperative interference management with MISO beamforming," *IEEE Trans. Signal Process.*, vol. 58, no. 10, pp. 5450–5458, 2010.
- [9] M. Mohseni, R. Zhang, and J. Cioffi, "Optimized transmission for fading multiple-access and broadcast channels with multiple antennas," *IEEE J. Sel. Areas Commun.*, vol. 24, no. 8, pp. 1627–1639, 2006.
- [10] E. Karipidis and E. Larsson, "Efficient computation of the Pareto boundary for the MISO interference channel with perfect CSI," in *Proc. WiOpt'10*, 2010, pp. 573–577.
- [11] E. Björnson, G. Zheng, M. Bengtsson, and B. Ottersten, "Robust monotonic optimization framework for multicell MISO systems," *IEEE Trans. Signal Process.*, vol. 60, no. 5, pp. 2508–2523, 2012.
- [12] A. Wiesel, Y. Eldar, and S. Shamai, "Linear precoding via conic optimization for fixed MIMO receivers," *IEEE Trans. Signal Process.*, vol. 54, no. 1, pp. 161–176, 2006.
- [13] E. Björnson, N. Jaldén, M. Bengtsson, and B. Ottersten, "Optimality properties, distributed strategies, and measurement-based evaluation of coordinated multicell OFDMA transmission," *IEEE Trans. Signal Process.*, vol. 59, no. 12, pp. 6086–6101, 2011.
- [14] W. Yu and T. Lan, "Transmitter optimization for the multi-antenna downlink with per-antenna power constraints," *IEEE Trans. Signal Process.*, vol. 55, no. 6, pp. 2646–2660, 2007.
- [15] V. Annapureddy and V. Veeravalli, "Sum capacity of MIMO interference channels in the low interference regime," *IEEE Trans. Inf. Theory*, vol. 57, no. 5, pp. 2565–2581, 2011.
- [16] H. Zhang, N. Mehta, A. Molisch, J. Zhang, and H. Dai, "Asynchronous interference mitigation in cooperative base station systems," *IEEE Trans. Wireless Commun.*, vol. 7, no. 1, pp. 155–165, 2008.
- [17] C. Studer, M. Wenk, and A. Burg, "MIMO transmission with residual transmit-RF impairments," in *Proc. ITG/IEEE WSA'10*, 2010.
- [18] H. Holma and A. Toskala, *LTE for UMTS: Evolution to LTE-Advanced*, 2nd ed. Wiley, 2011.
- [19] P. Zetterberg, "Experimental investigation of TDD reciprocity-based zero-forcing transmit precoding," *EURASIP J. on Adv. in Signal Process.*, vol. 2011, jan 2011.
- [20] Y. Huang and D. Palomar, "Rank-constrained separable semidefinite program with applications to optimal beamforming," *IEEE Trans. Signal Process.*, vol. 58, no. 2, pp. 664–678, 2010.
- [21] S. Boyd and L. Vandenberghe, *Convex Optimization*. Cambridge University Press, 2004.
- [22] M. Grant and S. Boyd, "CVX: Matlab software for disciplined convex programming," <http://cvxr.com/cvx>, Apr. 2011.
- [23] A. Wiesel, Y. Eldar, and S. Shamai, "Zero-forcing precoding and generalized inverses," *IEEE Trans. Signal Process.*, vol. 56, no. 9, pp. 4409–4418, 2008.
- [24] M. Schubert and H. Boche, "QoS-based resource allocation and transceiver optimization," *Foundations and Trends in Communication and Information Theory*, vol. 2, no. 6, pp. 383–529, 2005.